



The effect of vermiculite on the degradation and spallation of plasma sprayed thermal barrier coatings

M. Shinozaki, T.W. Clyne*

Department of Materials Science & Metallurgy, Cambridge University, Pembroke Street, Cambridge CB2 3QZ, UK

ARTICLE INFO

Article history:

Received 9 October 2012

Accepted in revised form 19 November 2012

Available online 27 November 2012

Keywords:

Thermal barrier coating (TBC)

Yttria-stabilized zirconia (YSZ)

Plasma spraying

Spallation

Vermiculite

Calcium-magnesia-alumina-silica (CMAS)

ABSTRACT

A study has been made of the effect of vermiculite (VM) on the sintering-induced spallation of plasma sprayed zirconia thermal barrier coatings (TBCs). The glass transition (~ 1040 °C) and melting (~ 1360 °C) temperatures of VM are representative of a broad class of so-called CMAS (calcium-magnesia-alumina-silica) particulates likely to be ingested into gas turbines. Selected loadings of VM powder were introduced onto the surface of free-standing coatings, followed by heating (1500 °C) for periods of up to 80 h. The presence of VM induces various microstructural changes in the coatings and also accelerates the rise in their (in-plane) Young's modulus. Finally, results are presented concerning the effect of VM on spallation resistance, using coatings sprayed onto dense alumina substrates. Spallation lifetimes can be substantially reduced by VM, even at relatively low levels (~ 1 wt.%). This is related to acceleration of the sintering-induced increases in coating stiffness.

© 2012 Elsevier B.V. All rights reserved.

1. Introduction

Thermal barrier coatings (TBCs) are widely used in various types of gas turbine [1,2]. They commonly comprise yttria stabilized zirconia (YSZ), on a metallic substrate, often with a bond coat of some sort. The function of the bond coat is to provide improved adhesion and to act as an oxidation barrier, by developing a protective oxide layer (a thermally grown oxide, TGO), often consisting predominantly of α -Al₂O₃. The two main methods of TBC deposition are plasma spraying (PS) and electron beam physical vapour deposition (EB-PVD). The focus of the current study is on PS TBCs. The microstructure of PS TBCs is composed of overlapping splats lying parallel to the substrate, with inter-lamellar pores, through-thickness intra-splat cracks and globular voids.

At high temperatures, including those commonly encountered under service conditions (~ 1000 – 1400 °C), there is a tendency for TBCs to undergo sintering. Modelling of the sintering process [3,4] has allowed prediction of associated microstructural changes in terms of shrinkage, surface area and porosity. It has also given insights into the creep rates within such coatings, which are relatively high at the temperatures concerned. It is well established that the associated stiffening can be pronounced [5–10]. A picture thus emerges of the coating being stress-free at the operating temperature, but in-plane stresses being created within it on cooling, due to the mismatch in thermal expansivity

between the YSZ ($\alpha_{\text{YSZ}} \sim 11 \times 10^{-6} \text{ K}^{-1}$) and the substrate ($\alpha_{\text{sub}} \sim 15 \times 10^{-6} \text{ K}^{-1}$). The misfit strain ($\Delta\alpha\Delta T$), perhaps allowing for some stress relaxation during cooling, is therefore typically of the order of a few millistrain. The stress levels that arise in the coating after cooling (to ambient temperature or thereabouts) thus vary from a few tens of MPa (for a typical as-sprayed coating stiffness of 10 GPa) to a few hundreds of MPa (when sintering has caused the stiffness to rise to 100 GPa). The associated strain energy release rates, for a coating with a thickness of 0.5 mm, rise from a few tens of J m^{-2} initially to a few hundreds of J m^{-2} when stiffening has occurred to this extent. A recently published paper [11] gives full details of the associated analysis, leading to a methodology for spallation lifetime prediction, based on the strain energy release rate reaching a critical value (the interfacial fracture energy).

It is also already clear that sintering, and the associated increases in stiffness, and hence in the driving force for spallation (debonding), can be (sharply) accelerated by the presence of calcium-magnesia-alumina-silica (CMAS) constituents [12–21], which can be ingested in the form of sand, volcanic ash, etc. This can cause dramatic increases in the rate of stiffening and hence can promote premature debonding. The present study is focussed on the effect of CMAS (at different levels) on stiffening of these coatings, and also on spallation lifetimes. This is done using a substrate (alumina) for which complications arising from changes in interfacial microstructure during the heat treatment are avoided. The thermal expansivity of alumina ($\alpha_{\text{alumina}} \sim 8 \times 10^{-6} \text{ K}^{-1}$) is lower than that of YSZ, so the misfit strain on cooling of a YSZ coating in this case is of the opposite sign to that of a superalloy substrate, but its magnitude is similar. Issues associated with such experiments being carried out using alumina substrates are covered in the previous paper [11]. In

* Corresponding author. Tel.: +44 1223334332; fax: +44 1223334567.
E-mail address: twc10@cam.ac.uk (T.W. Clyne).

the current study, the focus is on the effect of CMAS, represented by a particular naturally-occurring mineral (vermiculite). This has similarities to materials of particular interest, such as volcanic ashes, and also has the advantage that it is readily available and tends to exhibit little variation between samples from different sources.

2. Experimental procedures

2.1. Alumina substrate treatment and plasma spraying

In order to ensure good adhesion of the YSZ coating, the alumina substrates were roughened using a scanning laser beam (an SPI@ 200 W water-cooled fibre laser). Details of the procedures involved are given in a previous publication [11]. The surface roughness (R_a), measured using a Veeco Dektak 6M Stylus Profiler over a length of 5 mm, increased from $\sim 1.0 \mu\text{m}$ for the as-received substrates to $\sim 9.5 \mu\text{m}$ after laser-treatment.

The YSZ coatings were produced by plasma spraying of a standard (Sulzer NS-204) powder, using a VPS system with an F4 gun. Details are given elsewhere [11]. Coatings were sprayed onto alumina substrates with dimensions of $50 \times 50 \times 5 \text{ mm}$. After spraying, specimens were cut using a diamond wheel, with a slow feed rate, giving dimensions of $\sim 13 \times 10 \times 5 \text{ mm}$.

2.2. Examination of CMAS powder and YSZ coatings

Vermiculite (VM) is a hydrous silicate mineral and is widely mined for commercial uses such as for insulation panels or fertilizers. The VM powder was supplied by Goodfellows. The VM powder was subjected to a grinding operation and then sieved to give a selected size range. Its chemical composition, obtained from EDX data, is shown in Table 1. It is rich in Si and Mg, with traces of Al, Fe, K and Na.

Particle size distributions were obtained using a Malvern P580 Mastersizer E, adding the powders to an aqueous medium and keeping them in suspension using a stirrer. The plot is shown in Fig. 1. The average particle size is about $100 \mu\text{m}$. Of course, the size distribution is dependent on the sieving and grinding operations, and on mechanical characteristics of the powder particles, more than on their original sizes. Nevertheless, size distributions are relevant when considering the behaviour being studied here, and of course are also important in determining whether ingested particles adhere to blades etc. after impact.

Glass transition and melting temperatures were obtained using a Netzsch 404 DSC, with a ramp rate of $10 \text{ }^\circ\text{C min}^{-1}$, up to $1500 \text{ }^\circ\text{C}$. The DSC plot is shown in Fig. 2, where it can be seen that these temperatures are respectively $\sim 1040 \text{ }^\circ\text{C}$ and $1360 \text{ }^\circ\text{C}$.

The phases present in the VM powder, and in coatings exposed to VM, were investigated via X-ray diffraction measurements made using a Philips PW1710 diffractometer, with $\text{CuK}\alpha$ radiation ($\lambda = 0.154 \text{ nm}$), 40 kV accelerating current and a 40 mA filament current.

Table 1
Chemical composition (wt.%) of as-received VM powder, obtained from EDX data.

Element	Weight (%) Vermiculite
O	Bal.
Na	2.5
Mg	11.6
Al	4.0
Si	28.8
K	4.8
Ca	–
Ti	0.6
Fe	4.0

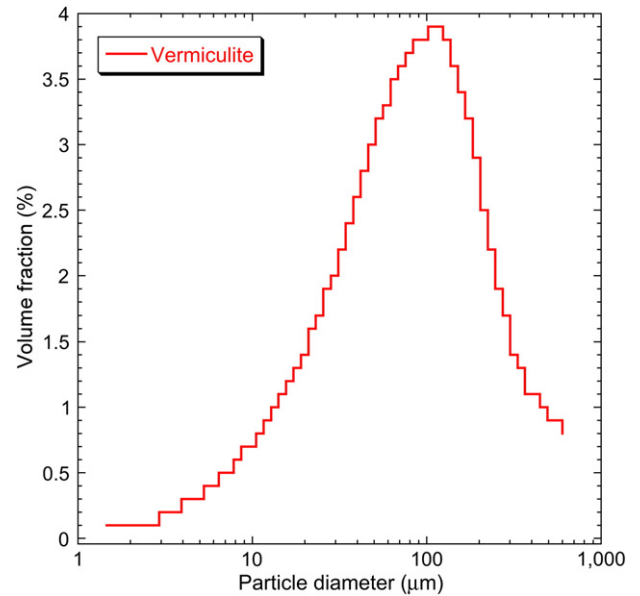


Fig. 1. Particle size distribution for VM powder after ball milling and sieving. Bin ranges are indicated by the widths of the histogram columns.

The XRD profile is shown in Fig. 3, where it can be seen that the VM powder contains only the expected vermiculite phase. It is important to note however that there is a prominent broad peak at around $20\text{--}30^\circ$ (2θ) which gives a clear indication that a substantial proportion of amorphous phase is present. The amorphous and crystalline phase proportions were calculated after peak deconvolution and profile fitting, performed using Phillips PROFIT software. The software can fit Lorentzian, Gaussian, pseudo-Voigt and Pearson-Seven profiles, all of which can be symmetrical or asymmetric. This procedure allows the determination of peak positions, peak areas and widths. The amorphous proportions of the VM sample were determined to be around 50%.

Coating microstructures were examined using a JEOL-5800 SEM, with a typical accelerating voltage of $10\text{--}15 \text{ kV}$. Samples were sputter coated with gold (using an Emitech 330 facility), to prevent charging.

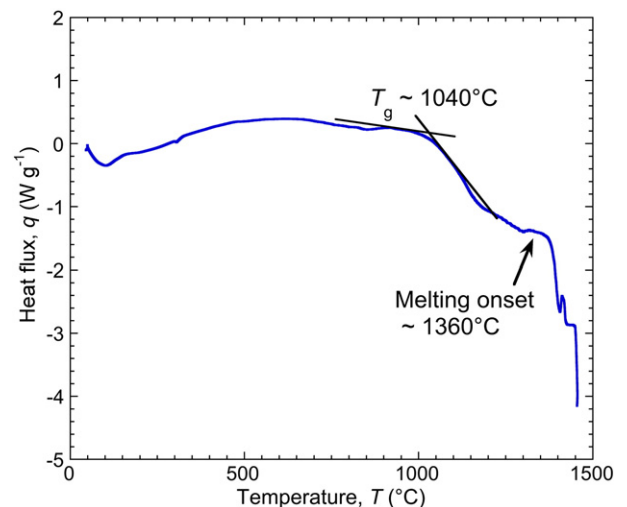


Fig. 2. Differential scanning calorimetry plot, obtained using a heating rate of $10 \text{ }^\circ\text{C min}^{-1}$, for the VM powder.

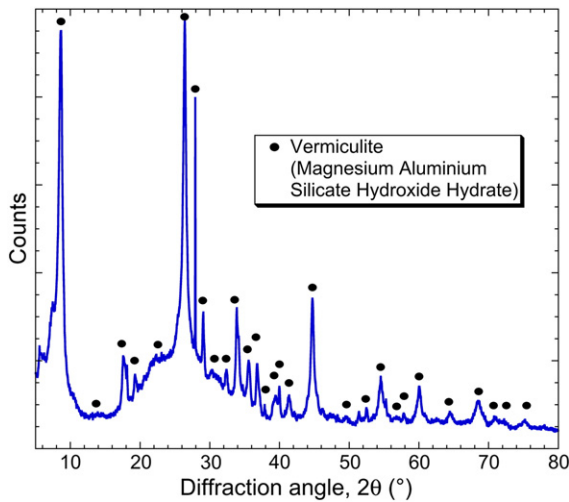


Fig. 3. X-ray diffraction scan from VM powder.

2.3. Application of CMAS powders to YSZ specimens

VM powder was applied onto the surface of free-standing YSZ coatings and also on specimens attached to alumina substrates, using the following steps:

- Spray adhesive was applied onto the surface of the YSZ coating
- VM powder was sprinkled on top
- The specimen was placed in a furnace held at 1200 °C for 10 min and allowed to air cool.

The free-standing YSZ specimens were obtained by spraying onto grit-blasted mild steel substrates. Detachment from the substrates was achieved by immersion in 36% HCl, which caused partial dissolution of the steel. Experiments were carried out in which such free-standing coatings were subjected to various heat treatments, parts of them being periodically cut off, polished, mounted and examined. SEM micrographs were taken of these sections, together with X-ray maps of elemental distribution, using a 30-minute accumulation time. Attention was largely focussed on the distribution of Si, which is virtually absent from the YSZ, but it is present at substantial levels in VM.

2.4. Coating stiffness measurement

Free-standing YSZ specimens were used to determine their stiffness as a function of heat treatment time and temperature. Heat treatments were conducted using a Lenton 1700 UAF 17/4 Furnace. Samples were located on a clean, flat alumina surface and placed inside the furnace once the set temperature had been reached. After heat treatment, they were taken out at high temperature and left to cool in air.

In-plane Young's modulus values were obtained via four point bending, using a scanning laser extensometer (Lasermike model 501-195, with a resolution of around 3 μm) to monitor specimen deflections. Specimen dimensions were approximately 15 × 100 × 0.6 mm. All measurements were made at room temperature. Loads were applied via a counter-balanced platen, using small pre-weighed masses.

2.5. Shrinkage during heat treatment

In-plane shrinkage of the YSZ coatings was monitored using a Netsch 402C dilatometer. The set-up comprises an alumina stage with an alumina push rod, which applied a constant load to the specimen (of 0.3 N). A linear variable displacement transducer (LVDT)

was used to measure the displacement of the push rod. Samples were held at 1400 °C and 1500 °C for 20 h. A calibration run was conducted in order to correct for dimensional change of the alumina push rod.

2.6. Periodic quenching and spallation monitoring

A computer-controlled furnace, with a periodic quenching capability, was used to investigate coating spallation. Details are given elsewhere [11]. Quenching (to approximately 100 °C) took place at hourly intervals, induced by 5 min of exposure to nitrogen jets. The system incorporates a webcam focussed on the sample boat, the output from which is recorded during quenching. Inspection of recorded images allowed the time of spallation to be established for individual specimens, without the need for frequent personal inspection. In this way, it is practicable to obtain data relating to substantial numbers of specimens, exhibiting relatively long spallation lifetimes.

3. Effect of VM deposits on coating microstructure

3.1. Ingress of VM into the coating

Fig. 4 shows BSE images of transverse polished cross sections of detached YSZ coatings, with 1.8 wt.% surface addition of VM, after different times at 1200 °C. Corresponding EDX maps for Si are also shown. These images suggest that the initial treatment leads to complete melting of the VM, followed by penetration into the (porosity within the) near-surface region of the coating. (Typical porosity levels in plasma sprayed YSZ, and also in those produced by PVD, are about 10–15 vol.%, with most of it being interconnected.) It seems likely that the liquid retains its integrity, although there are clear indications that a significant proportion of the surrounding zirconia dissolves in it. This of course is a well-known thermochemical interaction between YSZ and CMAS-type deposits, as outlined in [20]. For example, the depth of the liquid layer is apparently about 70–80 μm, whereas its thickness would be less than half that if it were composed solely of the original VM. Further evidence that the Si-rich region created initially (i.e. after 10 min) was composed of a mixture of liquid and residual crystalline zirconia is provided by the XRD scans shown in Fig. 5, obtained from the free surface of a specimen with 3 wt.% VM addition, after increasing times at 1200 °C. It can be seen that the initial profile exhibits a substantial broad peak (at 20–30° 2θ), reflecting the presence of an amorphous phase, plus the sharp peaks corresponding to (tetragonal) YSZ. Relative intensities broadly suggest something like 50% of each, which would require the dissolution of a substantial proportion of the original zirconia. These figures are very approximate, and it should be noted that the VM addition level was higher in the specimen used to produce the spectra in Fig. 5, compared with the one used to create Fig. 4, but the picture that emerges concerning the early stages of the process is a consistent one.

The other Si maps in Fig. 4 suggest that, after longer periods (1 h and 10 h), the Si-rich (i.e. the liquid) layer gradually disappears, presumably by diffusion of the species concerned into the rest of the coating. This method of monitoring the Si distribution is not suitable for the construction of an accurate composition profile, but it would appear that these species become homogeneously distributed throughout the coating fairly quickly. It seems likely that the diffusion takes place predominantly along the grain boundaries. The XRD profiles for the longer times shown in Fig. 5 also give some insights into the processes taking place. These show a reducing intensity of the amorphous peak – the amorphous content reduces from around 50% after 10 min down to 40% after 20 h – accompanied by increased intensities for the (tetragonal) zirconia peaks and also the appearance of some monoclinic zirconia peaks—for example at about 28° and 32°

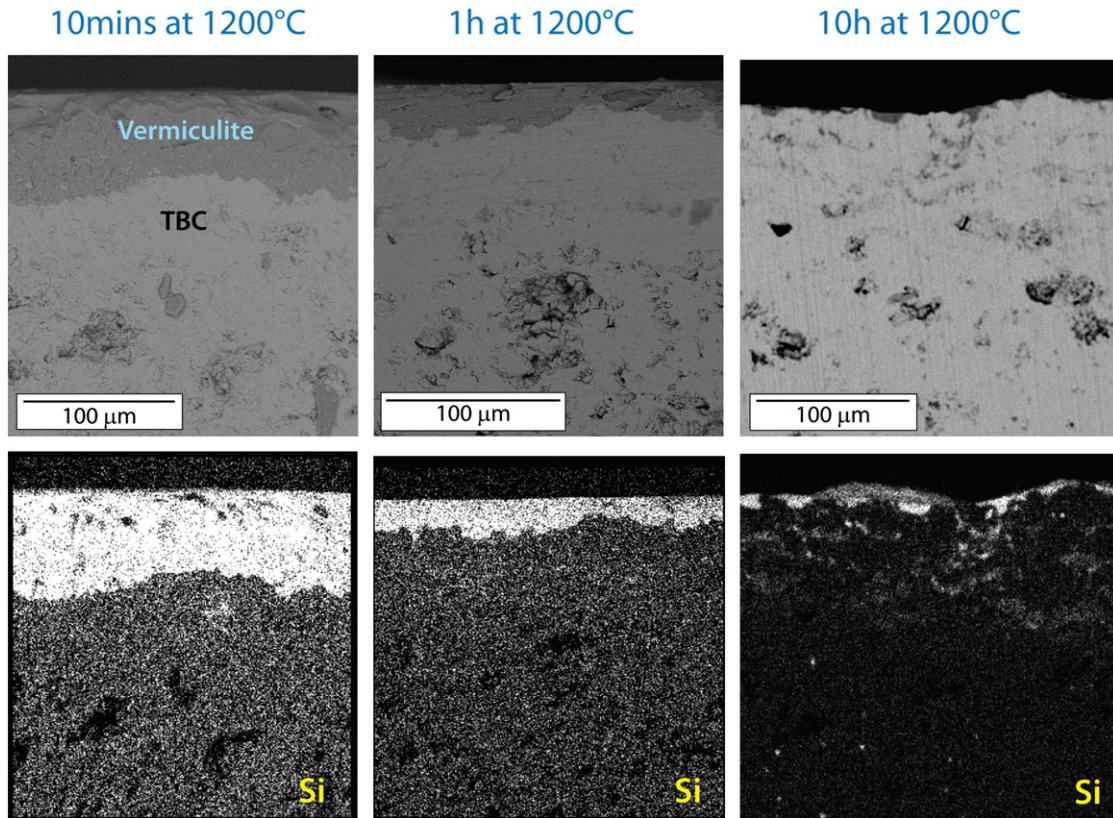


Fig. 4. Transverse section SEM (BSE) images of YSZ, with 1.8 wt.% surface addition of VM, after periods of 10 min, 1 h and 10 h at 1200 °C, and corresponding EDX maps showing the distribution of Si.

(2θ). This is consistent with a progressive penetration of species from the VM into the bulk of the coating, reducing the amount of residual liquid as its composition changes and zirconia crystallizes from it. It may be noted that no peaks appear corresponding to crystalline VM. However, a peak at around 27°, which may correspond to ZrSiO₄, appears after 20 h at 1200 °C. This peak cannot be indexed with any confidence. Other phases that might conceivably be responsible for

it include iron oxide, silicon oxide (quartz) and potassium zirconium silicate. However, it would not be surprising if ZrSiO₄ were to be formed, since it has been reported previously [19,22] to form during similar experiments.

Fig. 6 shows XRD profiles of YSZ, with 3 wt.% VM surface additions, after treatments of 5 h and 20 h at 1200 °C, from specimens subjected to mechanical polishing in order to remove the (partially)

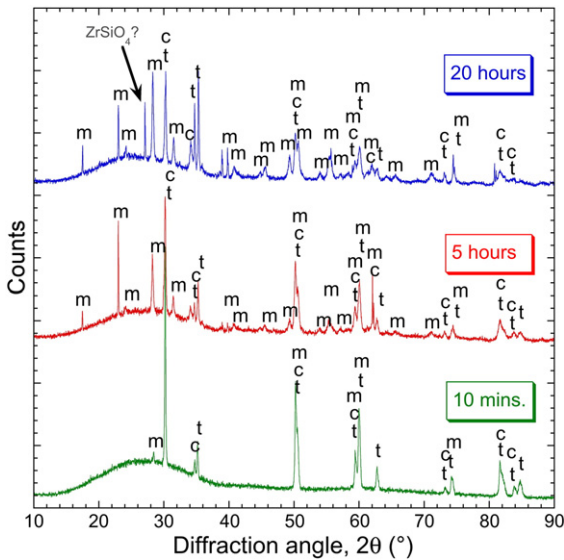


Fig. 5. XRD scans from the free surface of a YSZ specimen, with 3 wt.% VM surface addition, after different periods of holding at 1200 °C. The marked peaks correspond to monoclinic, tetragonal and cubic forms of zirconia, plus one that may be from zirconium silicate.

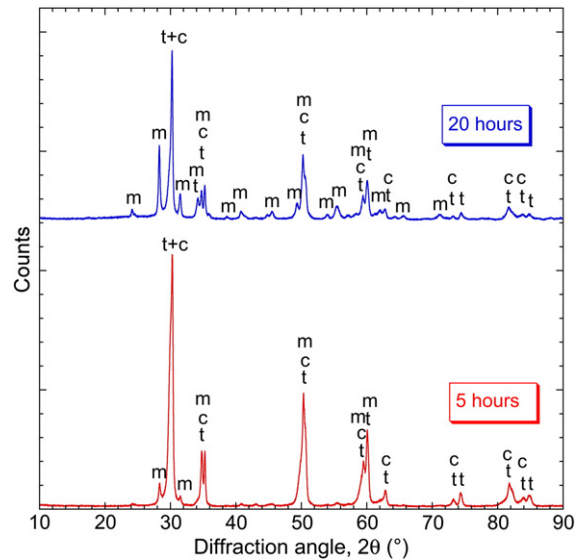


Fig. 6. XRD scans from the free surface of a YSZ specimen, with 3 wt.% VM surface addition, after 5 h and 20 h of holding at 1200 °C. These scans were obtained after the top glassy layer had been removed by polishing (to depths of, respectively, about 100 μm and 60 μm).

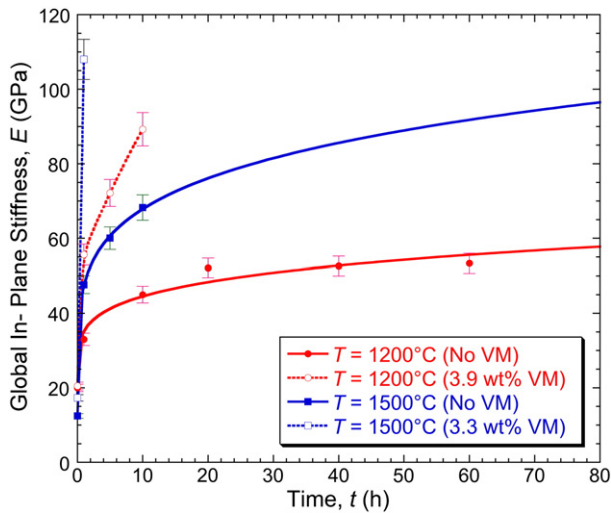


Fig. 7. Young's modulus data for free-standing YSZ coatings for samples with VM additions, at 1200 °C and 1500 °C. (The error bars represent standard deviations on sets of between 2 and 4 specimens in each case.)

glassy layer. These profiles indicate that, while the structure is fully crystalline (at that depth), some monoclinic zirconia does form. This is not unexpected, since it's known that high levels of impurity often promote formation of the monoclinic phase [20,21]. This observation is therefore consistent with species from the VM diffusing into the bulk of the coating.

3.2. Sintering-induced stiffening and shrinkage in the presence of VM

Young's modulus data for free-standing YSZ coatings, with and without surface additions of VM, are shown in Fig. 7. It's clear that VM substantially accelerates the rate of stiffening caused by sintering effects. This is particularly marked for when heat treated at 1500 °C, where there was probably a substantial amount of liquid present, and much of the sintering was liquid-assisted (ie involved viscous flow). These results are broadly consistent with the microstructural observations presented above.

Further information about the effect of VM additions on the behaviour at high temperature is provided by the plots in Fig. 8, which show dilatometry data. It can be seen that the in-plane shrinkage that accompanies sintering is considerably accelerated by the presence of

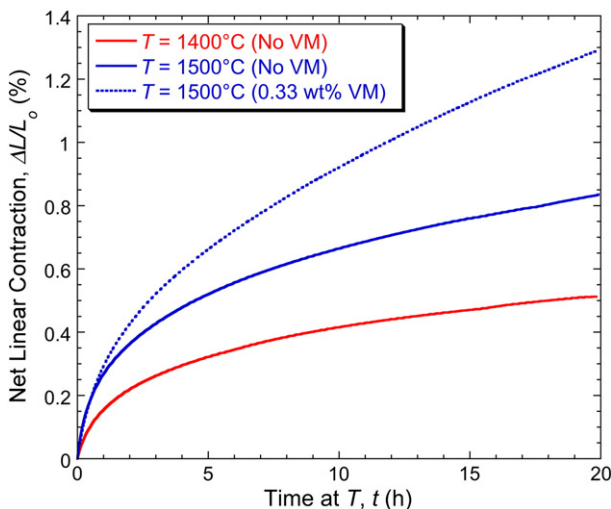


Fig. 8. Dilatometry data obtained during heating of free-standing YSZ coatings at 1400 °C, and also at 1500 °C (with and without VM additions).

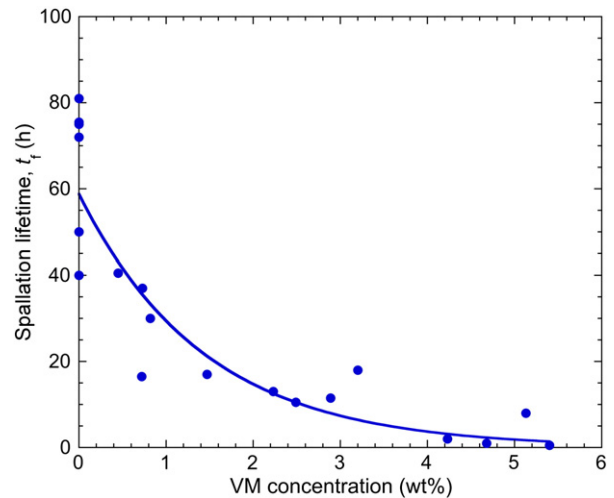


Fig. 9. Spallation lifetimes for YSZ coatings on alumina substrates, as a function of VM addition levels, for heat treatment temperatures of 1500 °C. Coating thickness for this set of results was about 750 μm.

the VM. It's worth noting that this shrinkage reflects only the effects of grain boundary diffusion—i.e. surface diffusion creates no shrinkage, although it can certainly contribute to sintering, and the associated stiffening [3,4]. The fact that the VM accelerates the shrinkage is consistent with its promotion of sintering being primarily due to enhanced grain boundary diffusion—probably caused by increasing the effective thickness of the grain boundaries.

4. Spallation lifetimes

Spallation lifetimes at 1500 °C, as a function of VM concentration, are shown in Fig. 9. It can be seen that even relatively low addition levels (<~1 wt.%) can have a pronounced effect in accelerating spallation at this (very high) temperature. This is consistent with the data in Fig. 7 and Fig. 8.

In a previous paper [11], a fracture mechanics based methodology was presented for estimation of the interfacial fracture energy from a measured spallation lifetime, knowing the coating stiffness as a function of time at the temperature concerned. In fact, for interfaces produced in the same way as in the current work, such spallation data (in the absence of VM) were employed to obtain an estimate of this fracture energy, which turned out to give a value of about $300 \text{ J m}^{-2} \pm 100 \text{ J m}^{-2}$. In the present work, a similar operation was carried out for a few spallation events—there were only two for which the stiffness as a function of time was available for the VM addition levels concerned. These data are presented in Table 2, where it can be seen that the estimated interfacial fracture energy was about 300–400 J m^{-2} . Of course, these values are very approximate, and based on minimal data, but it's nevertheless worth noting that they are similar to those obtained (from more systematic data) in the absence of VM. This is broadly as expected, since little change was evident in the interfacial microstructure after holding at elevated temperatures, with or without VM additions.

Table 2

Estimated values of the interfacial fracture energy (critical strain energy release rate), G_{ic} , from two spallation event lifetimes, in the presence of VM, using measured values of the coating stiffness as a function of time.

Spallation lifetime at $T = 1500 \text{ °C}$ (h)	VM level (wt.%)	Estimated E (GPa)	G_{ic}
2	4.2	199	468
1	4.7	108	241

5. Conclusions

The following conclusions can be drawn from this work.

- (a) A study has been undertaken of the effects that result from the addition of Vermiculite (VM), (considered to be representative of CMAS (calcia–magnesia–alumina–silica) type powders) to the free surfaces of plasma sprayed zirconia coatings, either free-standing or attached to an alumina substrate, followed by heat treatments (in the temperature range 1200–1500 °C). Attention has been focussed both on the microstructural changes induced as the powders melt and penetrate into the coatings and on the effects of the presence of the VM on sintering phenomena, and hence on the stiffness and shrinkage characteristics of the coatings, and on their spallation lifetimes when subjected to periodic quenching.
- (b) It has been found that VM powder penetrates rapidly into the coatings, such that, depending on the temperature, a layer is formed which is a mixture of liquid and residual zirconia, some of the original zirconia having dissolved in the liquid. This liquid-containing layer progressively becomes thinner as species within it diffuse into the coating, predominantly via the grain boundaries, and eventually the elements concerned become uniformly distributed throughout the coating. In fact, this tends to happen fairly quickly, apparently becoming complete, for example, in a few tens of hours at 1200 °C, for a coating thickness of about 500–700 µm and a CMAS addition level of a few wt.%.
- (c) This penetration of VM accelerates the sintering phenomena occurring within the coating, predominantly by promoting grain boundary diffusion. This gives rise to enhanced shrinkage and more rapid stiffening. Among the consequences of these changes is an increased likelihood of coating spallation from its substrate, if subjected to periodic quenching. This arises from the fact that, during cooling (from a stress-free condition at high temperature), creating a misfit strain as a result of differential thermal contraction, the resultant strain energy release rate (driving force for debonding) is raised by a stiffening of the coating.
- (d) It's clear that penetration of CMAS-type particulate has the potential to impair the thermo-mechanical stability of zirconia coatings. While the present work has been carried out only on plasma sprayed coatings, it seems likely that the conclusions apply equally to those produced by PVD techniques. Of course, this type of damage can only occur if particle impingement on the coatings causes them to adhere. However, this is

certainly possible under some circumstances, particularly if the powder has a relatively low melting temperature (and glass transition temperature), which is known to be the case for many volcanic ashes. It may be possible for coating formulations to be devised which improve their resistance to the microstructural changes responsible for enhanced sintering and spallation. Details presented here about these changes may be helpful in exploring the potential of this approach.

Acknowledgements

Funding for this work has come from a Schools Competition Act Settlement Trust (SCAST) Research Scholarship. The authors are very grateful to Kevin Roberts and Keith Page, of the Department of Materials Science in Cambridge University, for their extensive help with technical aspects of the spraying and the periodic quenching furnace. The assistance of Prof. Bill O'Neill and Dr. Martin Sparkes, of the Institute for Manufacturing in Cambridge University, with the laser processing of the alumina substrates, is also gratefully acknowledged.

References

- [1] X.Q. Cao, R. Vassen, D. Stöver, J. Eur. Ceram. Soc. 24 (2004) 1.
- [2] U. Schulz, C. Leyens, K. Fritscher, M. Peters, B. Saruhan-Brings, O. Lavigne, J.-M. Dorvaux, M. Poulain, R. Mevrel, M. Caliez, *Aerosp. Sci. Technol.* 7 (2003) 73.
- [3] A. Cipitria, I.O. Golosnoy, T.W. Clyne, *Acta Mater.* 57 (2009) 980.
- [4] A. Cipitria, I.O. Golosnoy, T.W. Clyne, *Acta Mater.* 57 (2009) 993.
- [5] M. Ahrens, S. Lampenscherf, R. Vassen, D. Stöver, *J. Therm. Spray Technol.* 13 (3) (2004) 432.
- [6] S.A. Tsipas, I.O. Golosnoy, R. Damani, T.W. Clyne, *J. Therm. Spray Technol.* 13 (3) (2004) 370.
- [7] J.A. Thompson, T.W. Clyne, *Acta Mater.* 49 (9) (2001) 1565.
- [8] S.R. Choi, D.M. Zhu, R.A. Miller, *J. Am. Ceram. Soc.* 88 (10) (2005) 2859.
- [9] F. Traeger, M. Ahrens, R. Vaßen, D. Stöver, *Mater. Sci. Eng., A* 358 (1–2) (2003) 255.
- [10] C. Pfeiffer, E. Affeldt, M. Göken, *Surf. Coat. Technol.* 205 (10) (2011) 3245.
- [11] M. Shinozaki, T.W. Clyne, *Acta Mater.* 61 (2) (2012) 579.
- [12] M.P. Borom, C.A. Johnson, L.A. Peluso, *Surf. Coat. Technol.* 87 (1996) 116.
- [13] C. Mercer, S. Faulhaber, A.G. Evans, R. Darolia, *Acta Mater.* 53 (2005) 1029.
- [14] S. Kramer, S. Faulhaber, M. Chambers, D.R. Clarke, C.G. Levi, J.W. Hutchinson, A.G. Evans, *Mater. Sci. Eng., A* 490 (2008) 26.
- [15] L. Li, N. Hitchman, J. Knapp, *J. Therm. Spray Technol.* 19 (January) (2010) 148.
- [16] X. Chen, *Surf. Coat. Technol.* 200 (2006) 3418.
- [17] J.M. Drexler, A.D. Gledhill, K. Shinoda, A.L. Vasiliev, K.M. Reddy, S. Sampath, N.P. Padture, *Adv. Mater.* 23 (21) (2011) 2419.
- [18] A.G. Evans, J.W. Hutchinson, *Surf. Coat. Technol.* 201 (2007) 7905.
- [19] A.D. Gledhill, K.M. Reddy, J.M. Drexler, K. Shinoda, S. Sampath, N.P. Padture, *Mater. Sci. Eng., A* 528 (24) (2011) 7214.
- [20] S. Kramer, J. Yang, C.G. Levi, C.A. Johnson, *J. Am. Ceram. Soc.* 89 (2006) 3167.
- [21] A. Aygun, A.L. Vasiliev, N.P. Padture, X. Ma, *Acta Mater.* 55 (2007) 6734.
- [22] P. Mechnich, W. Braue, U. Schulz, *J. Am. Ceram. Soc.* 94 (3) (2011) 925.